HELLENIC REPUBLIC
National and Kapodistrian University of Athens
EST. 1837

VIRTUAL 37th General Assembly of the European Seismological Commission
ESC2021 19-24 September 2021

# Destructive intensity inferred from strong ground motion recordings and its correlation with macroseismic intensity observations for the 2020 Samos Mw7.0, Greece, earthquake

Sakellariou N., Kouskouna V., Papadimitriou E., Karakostas V., Kassaras I.

# Introduction

- On 30 October 2020 11:51 UTC (13:51 local time) an earthquake of moment magnitude M7.0 occurred offshore the northern coast of Samos Island, in the Gulf of Ephesus/Kuşadasi.

- The earthquake reportedly caused 2 fatalities and 19 minor injuries at Samos Island, along with several injuries and significant damage to the building stock.

- In Western Turkey, the effects of the event were detrimental, with 116 fatalities, over 1,030 injuries and structural damage that included at least six collapses, in Izmir, approximately 70 km away from the epicenter

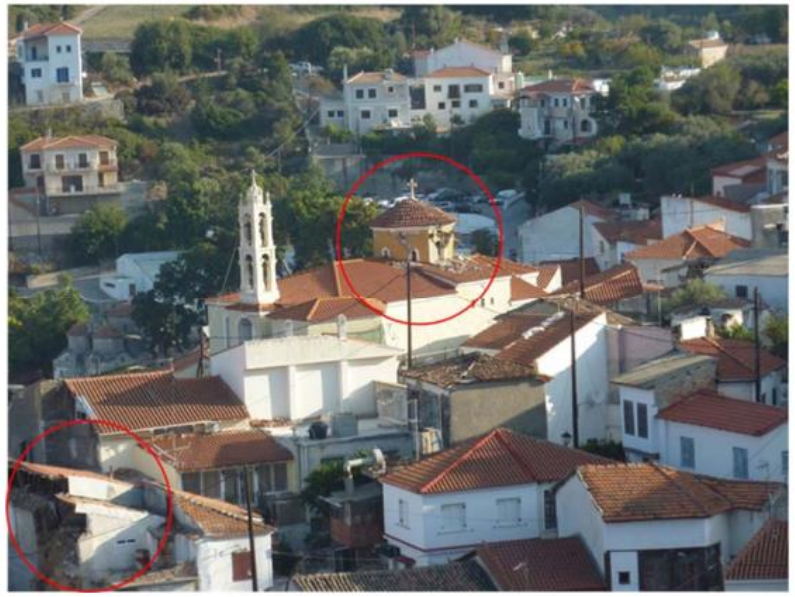

Fig. 1: Damages in Vathy

Fig.2: Damages in Izmir

# Regional Tectonic Setting - Seismotectonics

- The Aegean Sea and Western Anatolia are among the most seismically active areas in Eastern Mediterranean and have been the site of devastating earthquakes in both recent and historical times.

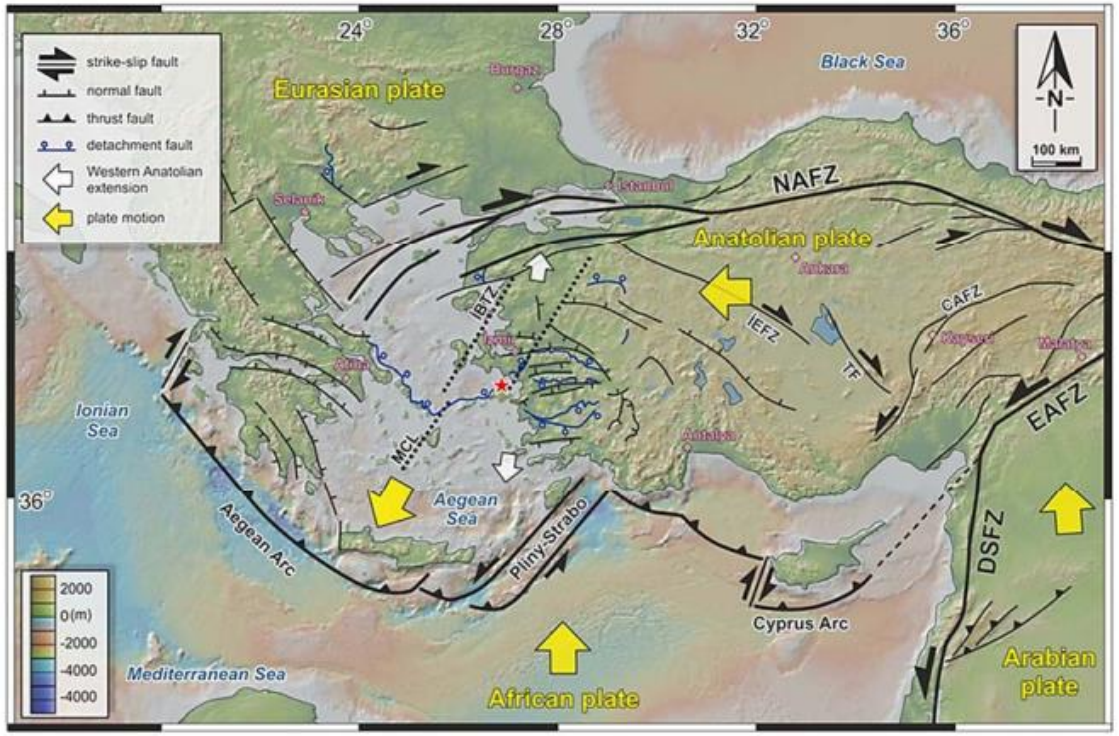


Fig.3: Tectonic setting of Eastern Mediterranean (modified from Uzel et al., 2013).

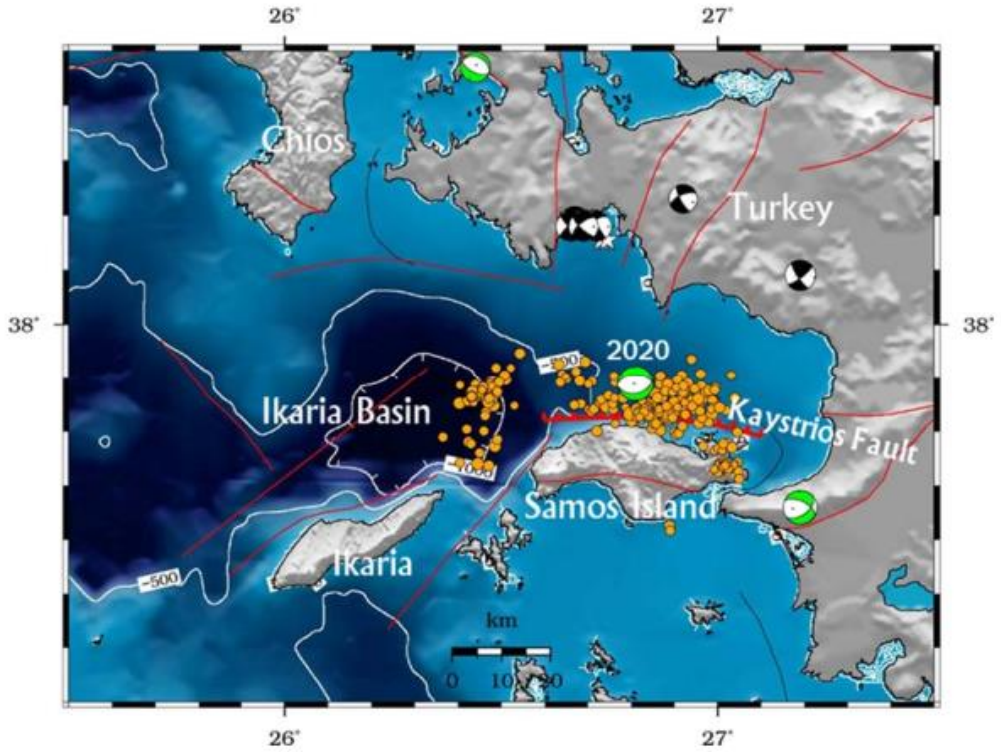


Fig.4: Relocated seismicity of M>3 (AUTh relocation) and mapped-inferred off-shore faults of the region (GreDAsSS, Caputo et al., 2012; Sboras, 2012).

# Regional Geology (Samos/Izmir)

- The geological succession on Samos island consists mainly of four distinct units. These refer to: (i) the Kerketeas marbles in the western part of the island, (ii) the Ampelos unit, which outcrops over the central part of the island, (iii) the Selçuk nappe, which crops out in the center area of the island as well, and (iv) the Vourliotes nappe which crops out in the eastern part of Samos.
- In the Turkish side, the metropolitan area of İzmir lies on the inner part of the bay, which is a morphological depression situated on the subsiding hanging wall block bounded by active normal faults from both sides.

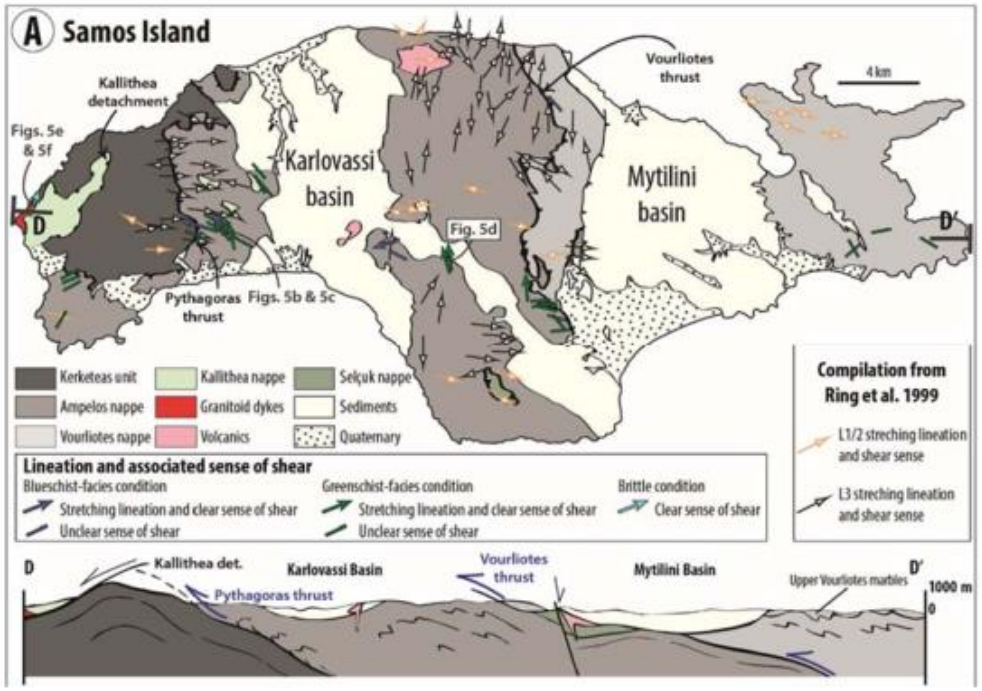


Fig.5: Simplified geological map of Samos (Roche et al. 2019)


Fig.6: Satellite view of İzmir Bay with geology (upper) (Uzel et al., 2013). A field photo of faults bounding İzmir Bay (lower).

# Historical Seismicity

- **Samos**

The earliest information for earthquakes in Samos dates back to 200BC, where information from inscriptions and historical reports (Bousquet and Pechoux, 1978; Taxeidis, 2003; Kouskouna, 2021) suggests the generation of a strong (M6.0-6.5) event, with significant impact on the island (I7-8).

The strongest event in antiquity is the 47AD, which caused heavy damage in Samos (I8) as well as in Izmir, Ephesus, Miletus and Chios (Papazachos and Papazachou, 2003).

- **Izmir**

The strongest event, in terms of intensity, occurred in 1688 near Izmir, most probably along the İzmir Fault. It caused heavy damage to the mosques, churches, and city walls. It caused a major fire in the city and caused over 2000 causalities (Pınar and Lahn, 1952).

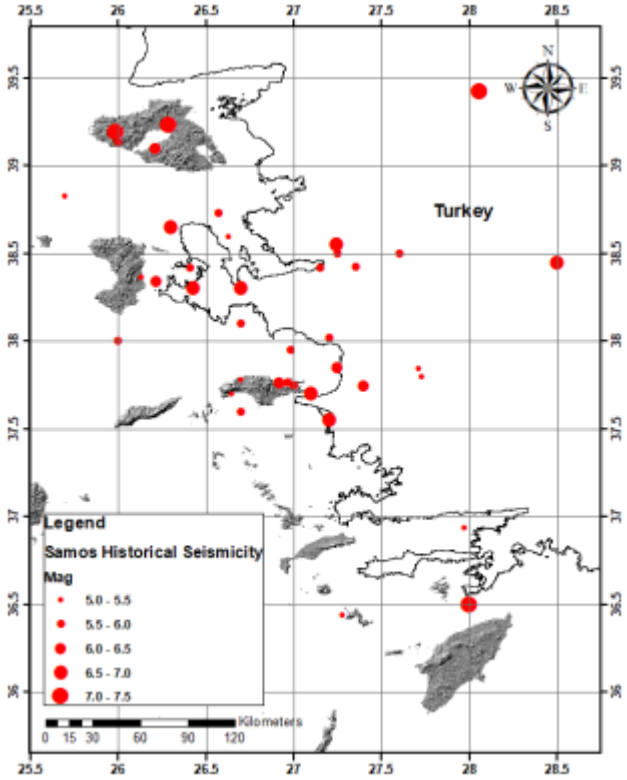


Fig. 7: Epicentral distribution of historical earthquakes with M≥5.0 in the broader Samos area during the period 1000-1899.

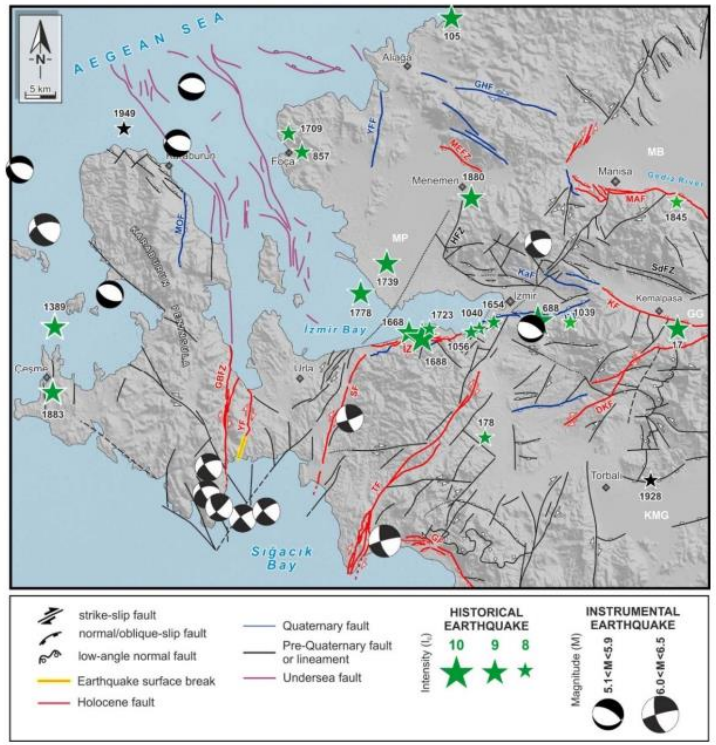


Fig. 8: Seismotectonic map of İzmir region. Faults are taken from Uzel et al. (2013) and Emre et al. (2018). Damaging historical earthquakes are compiled from Duman et al. (2016). Focal mechanisms of earthquake are taken from Tan et al. (2008).

# Definitions

- **Destructive Intensity (DI)** is defined as the logarithm of the absolute value of the inner product of the acceleration vector a (cm/s$^2$) and the velocity vector v (cm/s).

$$DI = \log\left(\sum |(\alpha * v)|\right)$$

- **Macroseismic Intensity (MI)** is an empirical measure of the earthquake effects at a certain place based on macroseismic observations discretisized and quantified through international scales

- The goal of this research is to correlate DI with MI, in order to define **Intrumental Intensity (II)**

# Methodology

- Calculation of DI in every strong motion station
- Matching MI in every station
- Correlation DI and MI
- Calculation of II
- Comparison between MI and II
- Localities where macroseismic intensity is assigned are considered phantom strong motion stations and synthetic strong motion recordings are calculated, using a stochastic finite source simulation approach, taking into account local soil conditions and topography.
- Maps showing the spatial distribution of II and MI are presented and compared

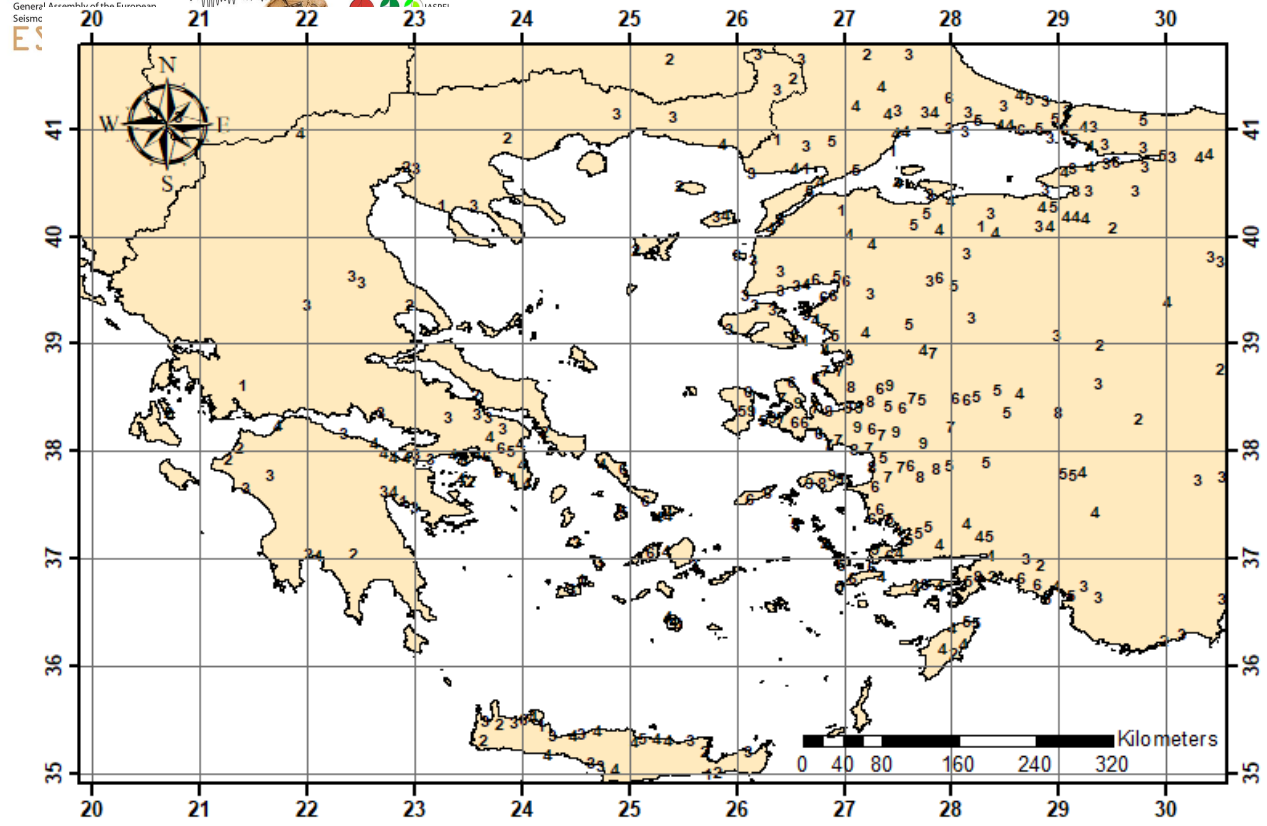


Fig. 9: Intensity spatial distribution

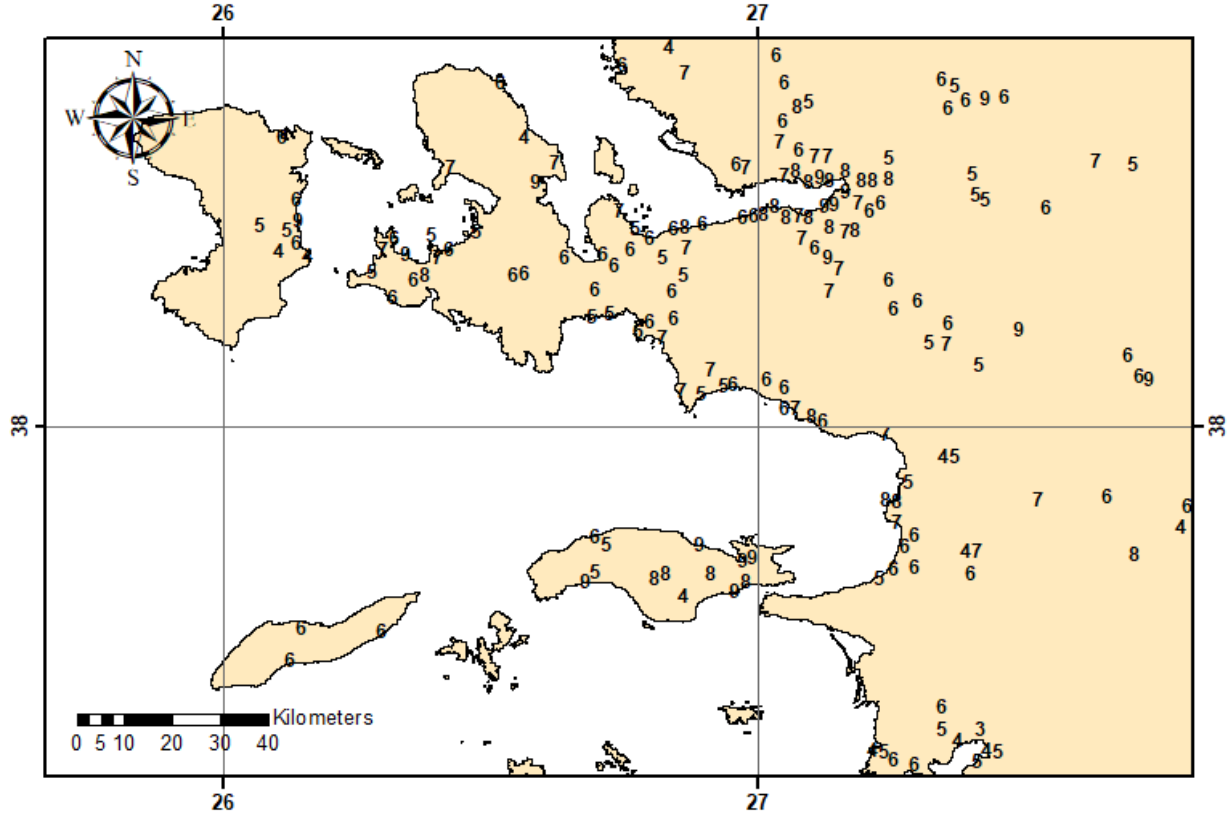


Fig. 10: Intensity spatial distribution for Samos and broader region

| Station | Lat | Long | PGA | PGV | I |
|---|---|---|---|---|---|
| SMG1 | 37.756 | 26.976 | 227.30 | 21.49 | 8 |
| SAMA | 37.754 | 26.981 | 166.31 | 16.00 | 8 |
| 905 | 37.860 | 27.265 | 179.31 | 7.85 | 8 |
| 911 | 37.762 | 27.391 | 66.66 | 4.54 | 6 |
| 918 | 37.370 | 27.264 | 38.19 | 5.99 | 6 |
| 919 | 37.560 | 27.836 | 21.40 | 1.22 | |
| 920 | 37.560 | 27.375 | 30.69 | 2.71 | 6 |
| 921 | 37.875 | 27.592 | 70.85 | 8.47 | 7 |
| 922 | 37.854 | 27.708 | 60.05 | 4.93 | 6 |
| 3506 | 38.394 | 27.082 | 43.88 | 3.39 | 7 |
| 3511 | 38.421 | 27.256 | 41.29 | 5.98 | 6 |
| 3512 | 38.401 | 27.152 | 57.54 | 3.31 | 6 |
| 3513 | 38.458 | 27.167 | 106.28 | 17.11 | 7 |
| 3514 | 38.476 | 27.158 | 56.02 | 6.41 | 6 |
| 3516 | 38.371 | 26.891 | 48.36 | 3.63 | 6 |
| 3517 | 38.376 | 27.194 | 40.10 | 3.95 | 8 |
| 3518 | 38.431 | 27.144 | 106.10 | 11.33 | 8 |
| 3519 | 38.453 | 27.111 | 150.09 | 22.53 | 8 |
| 3520 | 38.478 | 27.211 | 58.55 | 8.37 | 6 |
| 3521 | 38.468 | 27.076 | 110.84 | 16.17 | 7 |
| 3522 | 38.436 | 27.199 | 73.72 | 9.92 | 6 |
| 3523 | 38.328 | 26.771 | 80.32 | 5.73 | 6 |
| 3524 | 38.497 | 27.107 | 68.34 | 5.90 | 7 |
| 3526 | 38.578 | 26.980 | 88.77 | 10.82 | 7 |
| 3527 | 38.639 | 26.513 | 80.93 | 8.85 | 6 |
| 3528 | 38.304 | 26.373 | 149.31 | 8.36 | 7 |
| 3533 | 38.257 | 27.130 | 73.64 | 5.52 | 7 |
| 3534 | 38.662 | 26.759 | 92.48 | 4.91 | 6 |
| 3536 | 38.197 | 26.838 | 79.14 | 8.71 | 6 |
| 3538 | 38.319 | 27.123 | 85.48 | 5.48 | 7 |
| 3539 | 38.102 | 27.721 | 37.63 | 2.68 | 6 |
| 4501 | 38.613 | 27.381 | 40.00 | 6.81 | 6 |
| 4814 | 37.399 | 27.657 | 25.33 | 1.63 | |
| 4822 | 37.442 | 27.646 | 80.06 | 5.39 | |
| 4823 | 37.442 | 27.644 | 25.77 | 1.60 | |

Table 1: Available strong motion recordings within a range of 100Km

Table 2: Localities considered as phantom stations

| Locality | Lat | Long | I |
|---|---|---|---|
| Karlovasi | 37.795 | 26.707 | 9 |
| Samos | 37.752 | 26.982 | 9 |
| Kokkari | 37.778 | 26.891 | 9 |
| Karpovoulos | 37.694 | 26.951 | 9 |
| Karpovoulos | 37.692 | 26.955 | 9 |
| Kampos Marathokampou | 37.710 | 26.675 | 9 |
| Neo Karlovasi | 37.792 | 26.705 | 9 |
| Mesaio Karlovasi | 37.794 | 26.695 | 9 |
| Panayitsa | 37.756 | 26.979 | 8 |
| Mesogeio | 37.725 | 26.819 | 8 |
| Platanos | 37.721 | 26.978 | 8 |
| Pyrgos | 37.714 | 26.805 | 8 |
| Mytilinioi | 37.725 | 26.912 | 8 |
| Chios | 38.370 | 26.136 | 7 |
| Samos | 37.755 | 26.980 | 7 |
| Chios | 38.374 | 26.138 | 7 |
| Chios | 38.367 | 26.139 | 7 |
| Pigados | 37.065 | 25.192 | 6 |
| Tinos | 37.539 | 25.161 | 6 |
| Antimacheia | 36.803 | 27.092 | 6 |
| Mastichari | 36.828 | 27.086 | 6 |
| Piyi | 37.620 | 26.144 | 6 |
| Magganitis | 37.561 | 26.122 | 6 |
| Pyrgelia | 39.101 | 26.551 | 6 |
| Chios | 38.373 | 26.133 | 6 |
| Koumarionas | 37.748 | 26.976 | 6 |
| Palaiokastro | 37.738 | 26.999 | 6 |
| Kos | 36.893 | 27.288 | 6 |
| Marmaro | 38.543 | 26.107 | 6 |
| Varvasi | 38.363 | 26.136 | 6 |
| Agios Kyrikos | 37.615 | 26.294 | 6 |
| Chios | 38.371 | 26.133 | 6 |
| Messaria | 36.399 | 25.453 | 6 |
| Andros | 37.838 | 24.939 | 6 |
| Vrontados | 38.409 | 26.134 | 6 |

# Results

HELLENIC REPUBLIC
National and Kapodistrian University of Athens
EST. 1837

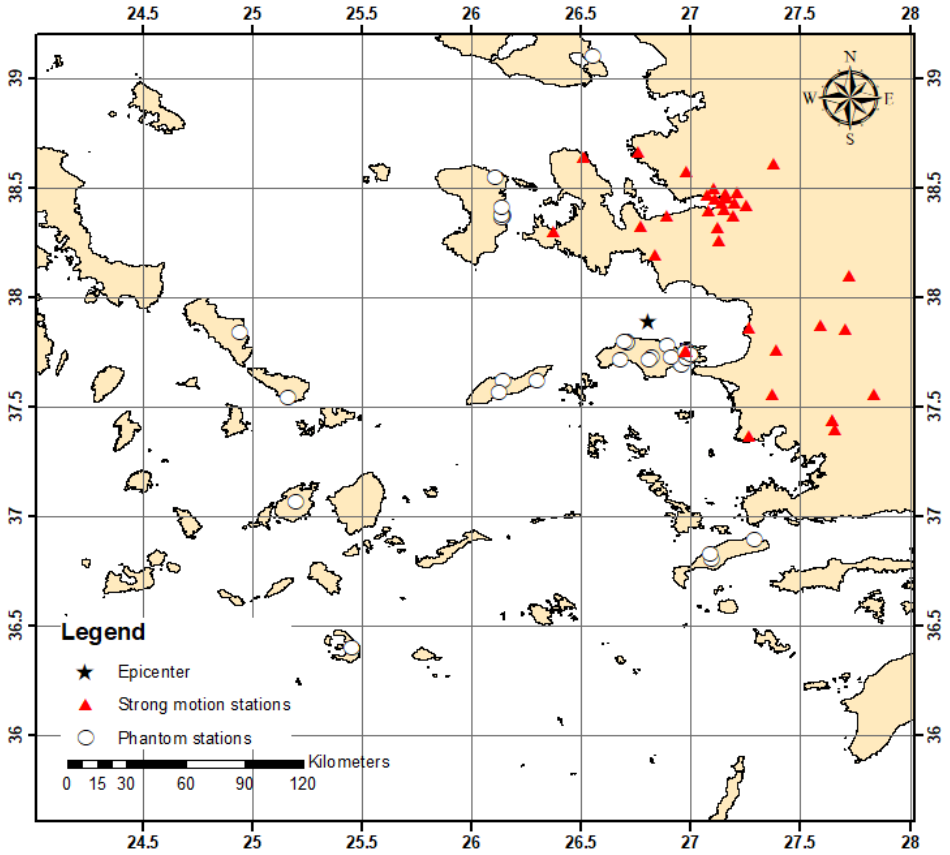


Fig. 11: Spatial distribution of strong motion and phantom stations

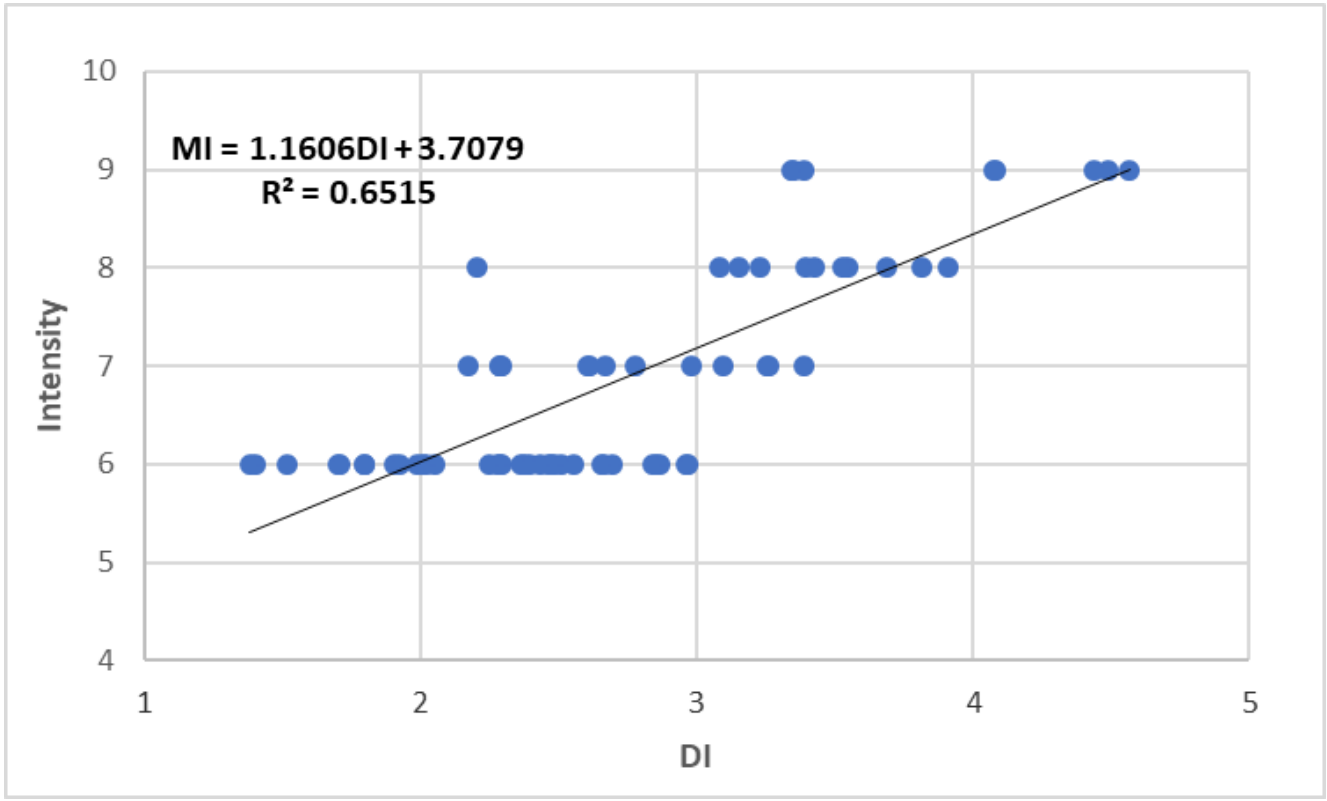


Fig. 12: Correlation of DI and MI

# Results

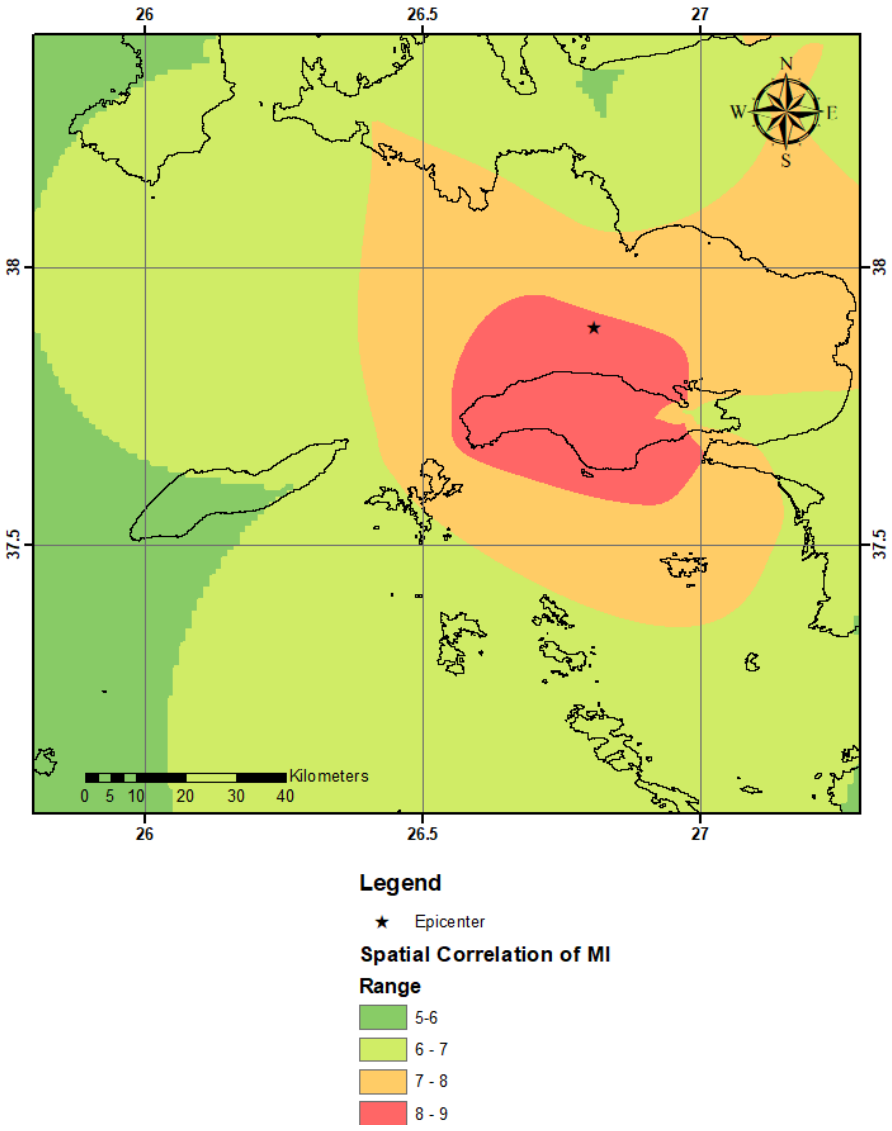


Fig. 13: Spatial correlation of MI

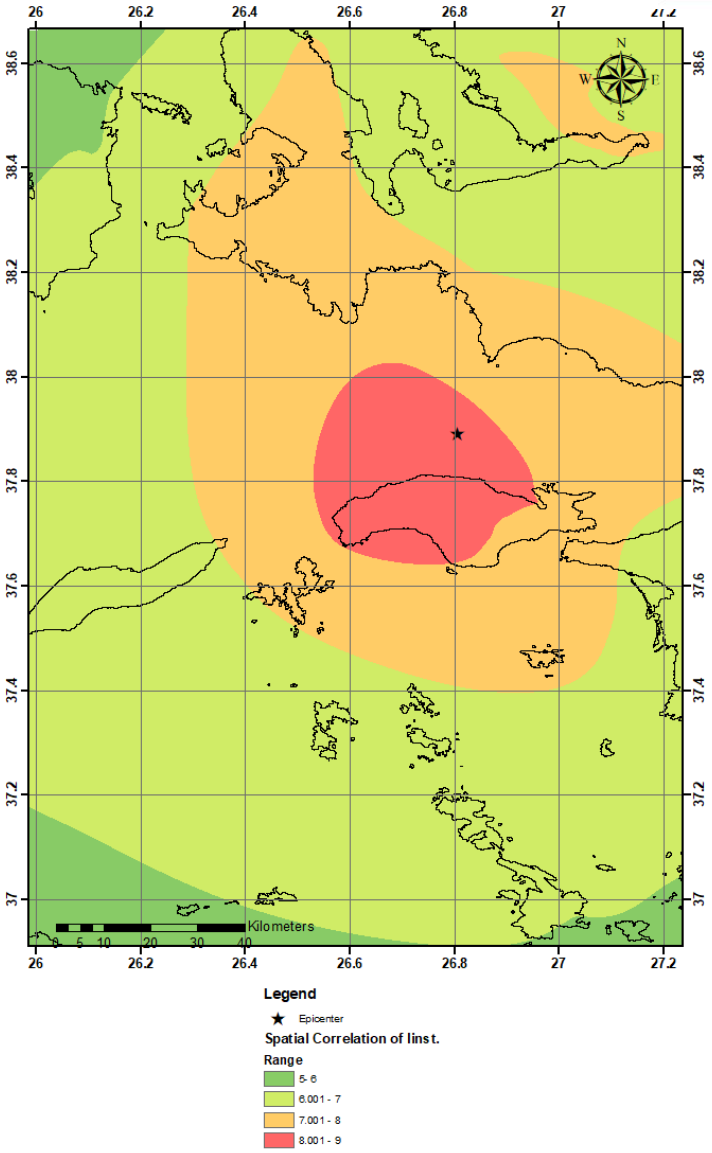


Fig. 14: Spatial correlation of II

# Conclusions

- On 30 October 2020 11:51 UTC (13:51 local time) M7.0 a destructive earthquake occurred offshore the northern coast of Samos Island (Kuşadasi [Ephesus] gulf), along a known normal fault (named North Samos or Kaystrios fault), previously identified on the basis of morphotectonic evidence, and confirmed by the earthquake generation.
- The information from the available historical seismicity suggests that similar magnitude events have previously occurred in the area.
- Regional geology and local soil conditions played significant role in the amplification of the energy, thus causing severe damage in Samos and Izmir.
- The earthquake was felt as far as Albania, to the North, south of Crete to the south and far east of the Minor Asia to the east.
- For the analysis we used strong motion recordings within 100Km.
- For all the other localities with MI≥6 synthetic waveforms were calculated, using the EXSIM (Boore, 2009).
- The overall number of synthetic waveforms were 35. The total available strong motion peak values were 66.
- Comparison of spatial correlation of MI and II shows similar pattern of energy release and damage distribution.

# THANK YOU FOR YOUR ATTENTION

# References


- Boore, D. M. (2009). Comparing stochastic point-source and finite-source ground-motion simulations: SMSIM and EXSIM. B of the Seismological Society of America, 99(6), 3202-3216.
- Bousquet, B. et Pechoux, PY, 1978. Recherches bibliographique sur la séismicité historique. Rapport Final D' ActivitéD'Activité Scientifique De L'EquipeÉquipe Du Laboratoire De Géologie Dynamique De L'Université Paris Sud Sur Le Résultat Des Etudes De Néotectonique en Grèce, 3, 47-65, 4, 93-126.
- Caputo, R, Chatzipetros A, Pavlides S. and Sboras S. 2012. The Greek Database of Seismogenic Sources (GreDaSS): state-of-the-art for northern Greece. Ann. Geophys, 55(5), 859-894.
- Duman, T.Y, Çan, T, Emre, Ö, Kadiroğlu, F.T, Başarır Baştürk, N, Kılıç, T, Arslan, S, Özalp, S, Kartal, R.F, Kalafat, D, Karakaya, F, Eroğlu Azak, T, Özel, N.M, Ergintav, S, Akkar, S, Altınok, Y, Tekin, S, Cingöz, A. and Kurt, A, 2017. Seismotectonic Map of Turkey with Explanations. General Directorate of Mineral Research and Explorations, Special Publication Series, 34, Ankara-Türkiye
- Emre, Ö, Duman, TY, Özalp, S, Şaroğlu, F, Olgun, Ş, Elmacı, H, and Can, T, 2018. Active fault database of Turkey. Bulletin of Earthquake Engineering, 16, 3229-3275.
- Nakamura, Y. (2004, August). On a rational strong motion index compared with other various indices. In 13th World Conference on Earthquake Engineering (pp. 1-6).
- Papazachos BC, and Papazachou C, 2003. The earthquakes of Greece. Ziti publications, Thessaloniki, Greece, 286 pp. (in Greek).
- Pınar, N. and Lahn, E, 1952. Türkiye'de zelzelelere müteallik etüdler. Publications of General Directorate of Mineral Research and Explorations B (5), 5–21.
- Roche V., Jolivet L., Papanikolaou D., Bozkurtf E., Menant A., Rimmelé G. (2019) Slab fragmentation beneath the Aegean/Anatolia transition zone: Insights from the tectonic and metamorphic evolution of the Eastern Aegean region, Tectonophysics 754: 101-129.
- Sboras S. 2012. The Greek Database of Seismogenic Sources: Seismotectonic implications for North Greece. PhD Thesis, University of Ferrara, Ferrara, 252 pp.
- Tan, O, Tapırdamaz, C. and Yörük, A, 2008. The Earthquake catalogues for Turkey. Turkish Journal of Earth Sciences, 17, 405–418.
- Uzel, B, Sözbilir, H, Özkaymak, Ç, Kaymakçı, N, Langeris, C.G, 2013. Structural evidence for strike-slip deformation in the İzmir-Balıkesir Transfer Zone and consequences for late Cenozoic evolution of western Anatolia (Turkey). Journal of Geodynamics, 65, 94–116.